BIOCHEMISTRY
including biophysical chemistry & molecular biology

Article

pubs.acs.org/biochemistry

# The Interaction between Eukaryotic Initiation Factor 1A and eIF5 Retains eIF1 within Scanning Preinitiation Complexes

Rafael E. Luna,[†,§] Haribabu Arthanari,[†,§] Hiroyuki Hiraishi,[‡,§] Barak Akabayov,[†] Leiming Tang,[‡] Christian Cox,[‡] Michelle A. Markus,[†,⊥] Lunet E. Luna,[†,¶] Yuka Ikeda,[‡] Ryosuke Watanabe,[‡] Edward Bedoya,[†] Cathy Yu,[†] Shums Alikhan,[†] Gerhard Wagner,*[,†] and Katsura Asano*[,‡]

[†]Department of Biological Chemistry and Molecular Pharmacology, Harvard Medical School, Boston, Massachusetts 02115, United States

[‡]Molecular, Cellular and Developmental Biology Program, Division of Biology, Kansas State University, Manhattan, Kansas 66506, United States

Supporting Information

**ABSTRACT:** Scanning of the mRNA transcript by the preinitiation complex (PIC) requires a panel of eukaryotic initiation factors, which includes eIF1 and eIF1A, the main transducers of stringent AUG selection. eIF1A plays an important role in start codon recognition; however, its molecular contacts with eIF5 are unknown. Using nuclear magnetic resonance, we unveil eIF1A's binding surface on the carboxyl-terminal domain of eIF5 (eIF5-CTD). We validated this interaction by observing that eIF1A does not bind to an eIF5-CTD mutant, altering the revealed eIF1A interaction site. We also found that the interaction between eIF1A and eIF5-CTD is conserved between humans and yeast. Using glutathione *S*-transferase pull-down assays of purified proteins, we showed that the N-terminal tail (NTT) of eIF1A mediates the interaction with eIF5-CTD and eIF1. Genetic evidence indicates that overexpressing eIF1 or eIF5 suppresses the slow growth phenotype of eIF1A-NTT mutants. These results suggest that the eIF1A−eIF5-CTD interaction during scanning PICs contributes to the maintenance of eIF1 within the open PIC.

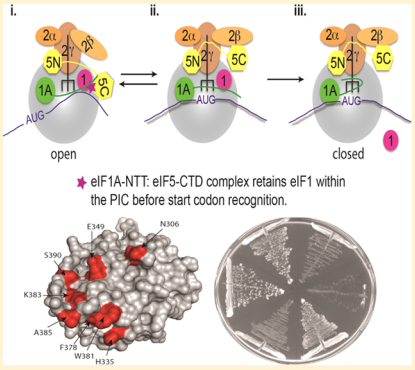


Accumulating evidence indicates that a sophisticated scanning system has evolved to efficiently locate the proper start codon on the mRNA in eukaryotes. This scanning process involves the dynamic interplay of translation initiation factors, ultimately regulating the conformational change of the ribosomal preinitiation complex (PIC).[1−5] To begin translation, the 40S small ribosomal subunit is preloaded with initiation factors eIF1A, eIF1, eIF2, eIF3, eIF5, and Met-tRNA$_i^{Met}$ in the 43S PIC.[4,6,7] The 43S PIC binds the 5′ end of the mRNA that had been primed by eIF4F and eIF4B and scans downstream until reaching a start codon.[8] The scanning PIC thus formed (43S PIC, which becomes 48S after it finds the start codon) is thought to exist in equilibrium between two conformations: open (scanning-competent) and closed (scanning-incompetent).[3,5] Once eIF1 and eIF1A have bound to the 40S subunit, these two initiation factors induce a conformational rearrangement of the 40S subunit from a closed to an open state.[9] During scanning, eIF1, eIF1A, and perhaps other assembled factors *in vivo*[10] facilitate the scanning of the PIC and prevent it from shifting to the closed state. Once the correct start codon is reached (with AUG in a proper sequence context), eIF1 is physically excluded from the decoding site, shifting the PIC into the closed conformation and arresting it at the start codon. Compared to bacterial initiation allowing the commencement of translation from UUG or GUG codons,[11] eukaryotic initiation strictly discriminates against these non-AUG codons.

Multiple eukaryotic initiation factors regulate the fidelity of start codon recognition by strictly coupling AUG recognition to the ribosomal conformational change.[12] It has been shown that overexpression of eIF1 increases the stringency of start codon recognition at its own AUG, which itself is in poor context,[13,14] whereas eIF5 overexpression reduces the stringency of start codon recognition at upstream open reading frames (uORFs) on its own mRNA.[15] These studies highlight the importance of understanding the mechanism by which eIF1, eIF1A, and eIF5 regulate the PIC conformations strictly in response to AUG base-pairing to the tRNA$_i^{Met}$ anticodon.

The structures of two domains of eIF5 have been determined by nuclear magnetic resonance (NMR) spectroscopy and X-ray crystallography. The first structural domain of eIF5 is the GTPase activating region located at the amino-terminal end (eIF5-NTD, residues 1−170).[16] The second structural domain is located at the carboxyl-terminal end (eIF5-CTD, residues 225−409) or eIF5-HEAT.[17] The HEAT domains were so named because of the structural resemblance of four proteins,

**Received:** July 21, 2013
**Revised:** December 5, 2013
**Published:** December 9, 2013

   dx.doi.org/10.1021/bi4009775 | *Biochemistry* 2013, 52, 9510−9518

all containing a series of $\alpha$-helices [Huntingtin, elongation factor 3 (EF3), the regulatory A subunit of protein phosphatase 2A, and TOR1 (a target of rapamycin)].[17−19] In yeast *Saccharomyces cerevisiae*, key eukaryotic initiation factors assemble off (or away) from the ribosome by forming the multifactor complex (MFC), consisting of eIF3, eIF5, eIF1, and the eIF2 ternary complex (TC).[6,20] Studies using yeast have shown that eIF5, in particular its CTD, serves a critical role in the assembly of the MFC via interactions with eIF1, eIF2$\beta$-NTD, and eIF3.[6,21] Mammalian eIF5-CTD has also been shown to directly bind to each of these partners.[17,22-24] In humans, a MFC similar to the yeast complex has also been observed.[7]

Previously, we showed that the CTD of eIF5 promotes start codon recognition by its dynamic interplay with eIF1 and subsequently eIF2$\beta$.[24] We provided evidence that the interaction of eIF2$\beta$ with eIF5-CTD drives the ribosomal PICs into the closed conformation by promoting the release of eIF1.[24] In this study, we propose that eIF1A plays a contributing role in supporting eIF1 in the open PIC through its interaction with eIF5-CTD. The amino terminal tail (NTT) of eIF1A was previously shown to increase initiation accuracy by promoting the closed conformation.[25,26]

On the basis of a previous study, the position of eIF1A-NTT indicates that it binds to the 40S subunit and could also interact directly with Met-tRNA$_i$, consistent with stabilization of the closed conformation.[27] However, it has been unclear how the NTT of eIF1A mediates its function within the open PICs prior to its closure on start codons. Interestingly, alanine substitution mutation *tif11*$^{17-21}$ altering amino acids 17−21 of the NTT of eIF1A displayed a slow growth phenotype as well as a strong PIC assembly defect, both of which were suppressed by overexpression of eIF1.[25] Thus, at least a part of the NTT of eIF1A is responsible for the retention of eIF1 within the scanning PICs (open state). Consistent with the additional role played by the NTT of eIF1A, this segment of eIF1A had been known to mediate the interaction with eIF2, eIF3, or eIF5.[28] In this study, our NMR spectroscopic data reveal that eIF1A interacts directly with the CTD of eIF5. Combining our results of biophysical and yeast genetic studies, we propose that the interaction between eIF1A and the CTD of eIF5 contributes to the retention of eIF1 in the open scanning compatible PIC *in vivo*.

## MATERIALS AND METHODS

**NMR Resonance Assignments and Chemical Shift Perturbation Assay.** NMR chemical shift mapping experiments were performed as described previously.[24,29] NMR spectra were recorded at 298 K on a Varian Inova 600 MHz spectrometer, equipped with a cryoprobe. Protein samples for NMR measurements contained 200 $\mu$M protein in buffer containing 200 mM NaCl, 20 mM Tris-HCl, 2 mM DTT, 1 mM EDTA, and 10% $D_2O$ (pH 7.2). We utilized the backbone resonance assignments of human eIF5-CTD.[24]

**Small-Angle X-ray Scattering (SAXS) Reconstitution Assay.** SAXS experiments were performed as previously described.[24,30] Briefly, SAXS is a biophysical method that uses the elastic scattering of X-rays to probe sample features in a nanometer scale. SAXS allows the characterization of structure and interactions of macromolecules and their complexes in solution. Protein samples were measured in 20 mM Tris-HCl (pH 7.4), 300 mM NaCl, and 0.5 mM TCEP. SAXS experiments were performed for the following protein samples: (1) eIF5-CTD, (2) eIF1A, and (3) eIF1A−eIF5-CTD complex. eIF5-CTD was at a final concentration of 90 $\mu$M, while eIF1A titration concentrations were 90, 180, and 360 $\mu$M. As a control, the concentration of eIF1A alone was 180 $\mu$M. The $R_g$ values for eIF5-CTD, in the free state and in the eIF1A-bound state, were derived from SAXS intensities and determined using Guinier analysis.

**Construction of Plasmids.** All of the plasmids used for NMR and SAXS experiments are bacterial expression vectors encoding human initiation factors that contain either N-terminal or C-terminal hexahistidine tags. The proteins were purified as previously described.[24] Briefly, the initiation factors were purified through standard Ni-NTA columns and subsequent gel filtration. The peak fractions were collected and tested for the presence of the target protein using sodium dodecyl sulfate−polyacrylamide gel electrophoresis followed by staining with Coomassie blue. The human eIF5 plasmid clone encodes eIF5-CTD amino acid residues 225−409 with a C-terminal $His_6$ tag. $His_6$-tagged human eIF1A constructs were kindly provided by A. Marintchev. The expression construct for the yeast eIF5-CTD clone (TIF5-B6$_{241-405}$) was described previously.[31] pET-TIF11, the expression plasmid for yeast eIF1A, was constructed by cloning a 0.4 kb NdeI−BglII fragment of pGAD-TIF11 [pKA129 (from K. Asano, personal stock)] into the NdeI and BamHI sites of pET15b. For eIF5 overexpression, we subcloned the 2.2 kb EcoRI−HindIII *TIF5* fragment of YEpL-TIF5, YEpL-TIF5-7A,[32] or YEpL-TIF5-Quad[24] into YEplac112 to generate YEpW-TIF5, YEpW-TIF5-7A, or YEpW-TIF5-Quad, respectively. These plasmids overproduce wild-type or mutant versions of C-terminally FLAG-tagged yeIF5.

**Yeast Genetic Experiments.** Yeast genetic experiments and reporter assays were performed as described previously.[33] Strains KAY955 (*TIF11*), KAY956 (*tif11*$^{7-11}$), and KAY957 (*tif11*$^{12-16}$) were constructed by transforming H3582 (*tif11*Δ p[*URA3 TIF11*]) with *LEU2 FL-TIF11* plasmid pDSO157, its *tif11* derivatives, pCF84, and pCF85,[25] respectively, and evicting the *URA3 TIF11* plasmid in H3582 by 5-fluoroorotic acid (plasmid shuffling). To overexpress eIF1, we used pCF82 (2$\mu$ *TRP1 SUI1*) (A. G. Hinnebusch, personal collection) or YEpU-SUI1 (2$\mu$ *URA3 SUI1*).[34] Assays of $\beta$-galactosidase activity in whole cell extracts (WCEs) were performed as described previously.[33]

## RESULTS

**eIF1A Interacts with eIF5-CTD at a Site That Is Targeted by eIF2$\beta$-NTT and Overlaps the eIF1-Binding Surface.** eIF5-CTD interacts with eIF1 and eIF2$\beta$-NTT at overlapping but distinct surfaces.[24] In this study, we employed an NMR chemical shift perturbation assay to study the interaction of heIF1A with heIF5-CTD. The domain organization of these factors and the constructs used in this work are shown in Figure 1A. The NMR chemical shift perturbation (CSP) assay exploits the sensitivity of the chemical shift of a nucleus to its environment (reviewed in ref 29). To determine whether the interaction of heIF5 with heIF1A occurs through the amino-terminal domain (NTD) of heIF5, we used the CSP assay. However, we found no interaction between these two proteins (Figure S1 of the Supporting Information). We were also not able to detect an interaction between heIF1A and heIF1 (Figure S2 of the Supporting Information).


dx.doi.org/10.1021/bi4009775 | *Biochemistry* 2013, 52, 9510−9518

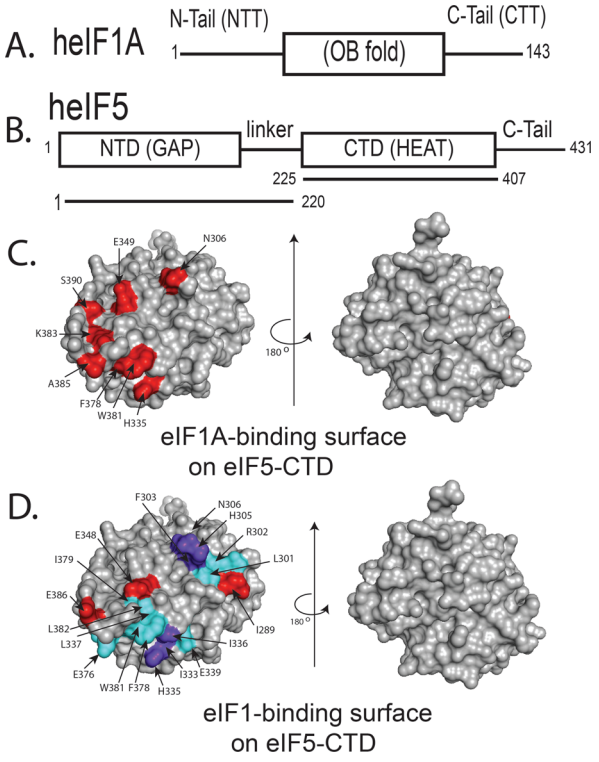


**Figure 1.** eIF1A and eIF1 bind to overlapping but distinct binding surfaces on eIF5-CTD. (A) Domain organization of eIF1A. Abbreviations: NTT, amino-terminal tail; CTT, carboxyl-terminal tail; OB (oligonucleotide/oligosaccharide) fold domain structured as an elliptically shaped $\beta$-barrel. (B) Domain organization of eIF5. Abbreviations: NTD, amino-terminal domain; GAP, GTPase-activating protein; CTD, carboxyl-terminal domain. eIF5-CTD is a member of the HEAT domain family consisting of a series of $\alpha$-helices. (C) NMR mapping of the heIF1A-binding surface on heIF5-CTD (Protein Data Bank entry 1IU1). Contacts are observed on only one face of the domain. heIF5-CTD residues for which heIF1A causes chemical shift perturbations (CSPs) are colored red. Two orientations of the heIF5-CTD molecule are shown as surface representations: (left) interaction interface and (right) a rotation of 180° along the *Y*-axis that shows no interaction on the other side of the molecule. The left molecule of heIF5-CTD is in an orientation similar to that of the molecule in panel D. (D) NMR mapping of the heIF1-binding surface on heIF5-CTD was adapted from our previously published study, in which the residues colored red experience CSPs, the residues colored cyan are broadened because of paramagnetic relaxation enhancement (PRE) experiments, and residues colored purple experience both PRE-induced broadening and CSPs:[24] (left) interaction interface and (right) a rotation of 180° along the *Y*-axis that shows no interaction on the other side of the molecule.

As shown in Figure 1C, we discovered a novel interaction between heIF1A and heIF5-CTD. On the NMR time scale, this interaction is in the intermediate exchange regime. At physiological salt concentrations of 150 mM NaCl, addition of heIF1A to $^{15}$N-labeled heIF5-CTD completely broadens the spectrum with the exception of the few unstructured residues. However, increasing the salt concentration weakens the interaction between heIF5-CTD and heIF1A, thereby pushing it toward a fast exchange regime. This is reflected in the appearance of resonances in the structured region of the heIF5-CTD spectrum at NaCl concentrations of 200 and 300 mM (Figure S3 of the Supporting Information). At a NaCl concentration of 300 mM, we were able to monitor chemical shift perturbations and map the binding of heIF1A (Figure S4 of the Supporting Information).

We found that the eIF1A-binding site involves residues (F378, W381, K383, A385, and S390) closely overlapping with the eIF2$\beta$-binding site. The addition of unlabeled eIF5-CTD significantly broadened the resonances of [$^{15}$N]eIF1A (Figure 2B, left panel), which may be due to a larger size resulting from complex formation, from multiple bound conformations, or from the reduced solubility of the formed complex. Utilizing our previously characterized quadruple mutation (H305D/N306D/E347K/E348K), by which one face of eIF5-CTD is altered to disrupt its interaction with eIF1 and eIF2$\beta$, we discovered that the eIF5-CTD-Quad mutant significantly

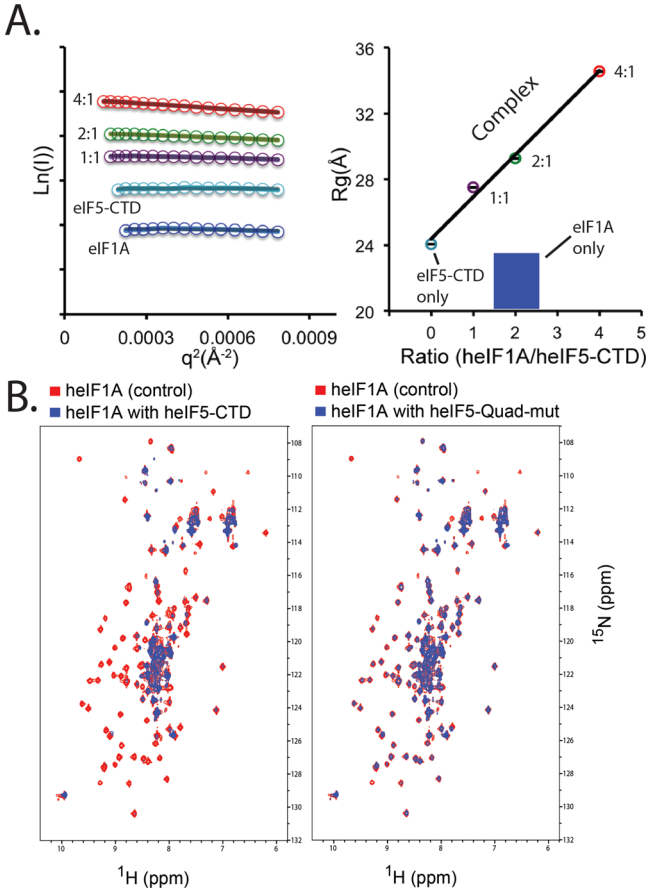


**Figure 2.** SAXS and NMR experiments indicate that eIF1A binds eIF5-CTD, while the eIF5-CTD-Quad mutant significantly weakens the interaction with eIF1A. (A) SAXS Guinier plots (left) shown for different heIF1A:heIF5-CTD molar ratios with the color codes used in the right panel. SAXS results (right) used to plot the radius of gyration ($R_g$) (*Y*-axis) vs heIF1A:heIF5-CTD protein ratio (*X*-axis). The $R_g$ was derived from the Guiner plots (left). $R_g$ serves as an indicator of the formation of higher-order protein complexes. To exclude the possibility that the $R_g$ is increased solely because of the higher concentration of heIF1A, we used a higher concentration of heIF1A alone [180 $\mu$M (blue)] as a control. Cyan corresponds to heIF5-CTD alone (90 $\mu$M). Data were collected for heIF5-CTD [90 $\mu$M (cyan circle)] titrated with increasing amounts of heIF1A [90 $\mu$M (purple), 180 $\mu$M (green), and 360 $\mu$M (red)]. (B) Overlay of $^{1}$H−$^{15}$N HSQC spectra (left) of 0.2 mM $^{15}$N-labeled heIF1A alone (red) and in the presence (blue) of 0.4 mM unlabeled wild-type heIF5-CTD domain. Overlay of $^{1}$H−$^{15}$N HSQC spectra (right) of 0.2 mM $^{15}$N-labeled heIF1A alone (red) and in the presence (blue) of 0.4 mM unlabeled heIF5-CTD-Quad mutant.


dx.doi.org/10.1021/bi4009775 | *Biochemistry* 2013, 52, 9510−9518

weakens the interaction of eIF5 with eIF1A (Figure 2B, right panel). We previously identified the heIF1-binding surface on heIF5-CTD (Figure 1D); however, its binding affinity could not be determined. In contrast, the affinity between heIF5-CTD and heIF2$\beta$-NTT was ~17 $\mu$M.[24] Given the proximity of eIF1 and eIF1A within the PIC,[27,35−38] it is reasonable to postulate that the CTD of eIF5 bridges the interaction between eIF1 and eIF1A.

**The SAXS Reconstitution Assay Shows That eIF1A and eIF5-CTD Interact.** We employed an alternative approach to show that heIF1A binds heIF5-CTD. As an orthogonal binding assay to NMR, we used small-angle X-ray scattering (SAXS) to monitor the weak binding interaction of the heIF1A−heIF5-CTD complex in solution, which was also used previously to characterize the binding between heIF1 and heIF5-CTD.[24] In this SAXS reconstitution assay, increasing amounts of heIF1A were titrated into a fixed concentration of heIF5-CTD, and the mixture at each point was subjected to SAXS analysis. In this assay, the radius of gyration ($R_g$) reflects the conformational/binding state of the proteins in solution, either free or in complex with each other.[24,30] Titrating heIF1A into a solution with a fixed concentration of heIF5-CTD results in a steady increase in $R_g$, consistent with formation of the complex between heIF1A and heIF5-CTD (Figure 2A, colored lines, left panel, and colored spheres, right panel). Free heIF1A (high concentration) has an $R_g$ value of 23.1 Å. At the same concentration of heIF5-CTD in the presence of twice the amount of heIF1A (2:1 molar ratio), the $R_g$ value is dramatically increased to 29.3 Å, indicating complex formation. A large amount of eIF1A alone (180 $\mu$M) did not increase the $R_g$, indicating that this increase is not due to interparticle interference. The results support the notion that heIF1A binds weakly to heIF5-CTD, because formation of the complex did not reach saturation even though we added a large excess of the heIF1A titrant. A similar observation was made in the SAXS study of the eIF1−eIF5-CTD complex.[24]

**The Interaction between eIF1A and eIF5-CTD Is Evolutionarily Conserved.** Our data clearly show that eIF1A interacts with eIF5-CTD. The eIF1A amino acid sequence alignment shows a striking similarity of basic residues (lysines and arginines) within the NTT regions of human and yeast eIF1A (Figure 3A). We assessed whether yeast eIF5-CTD (amino acids 241−405; Tif5p-B6) also interacted with yeast eIF1A (Tif11p or yeIF1A), which has not been previously assessed. In the left panel of Figure 3B, we show that yeast eIF5-CTD (Tif5p-B6) does bind to yeIF1A; hence, the eIF1A−eIF5-CTD interaction is conserved between human and yeast proteins. We proceeded to evaluate whether the heterologous proteins could bind each other. In the middle panel of Figure 3B, we noticed that $^{15}$N-labeled yeIF1A (Tif11p) binds to unlabeled human eIF5-CTD, as evidenced by chemical shift perturbations and peak broadening. We evaluated whether $^{15}$N-labeled yeIF1A (Tif11p) would bind to the human eIF5-CTD-Quad mutant protein. In the right panel of Figure 3B, we clearly see weakened binding between $^{15}$N-labeled yeIF1A (Tif11p) and the human eIF5-CTD-Quad protein, as evidenced by the return of the previously broadened signals in the spectra and significantly less chemical shift perturbation, compared to that seen in the middle panel of Figure 3B. Hence, yeast eIF1A binds to the face on the human eIF5-CTD molecule that binds to human eIF1A. Because yeast eIF1A binds to yeast eIF5-CTD protein and heterologously with human eIF5-CTD, we suggest that the eIF1A−eIF5-CTD

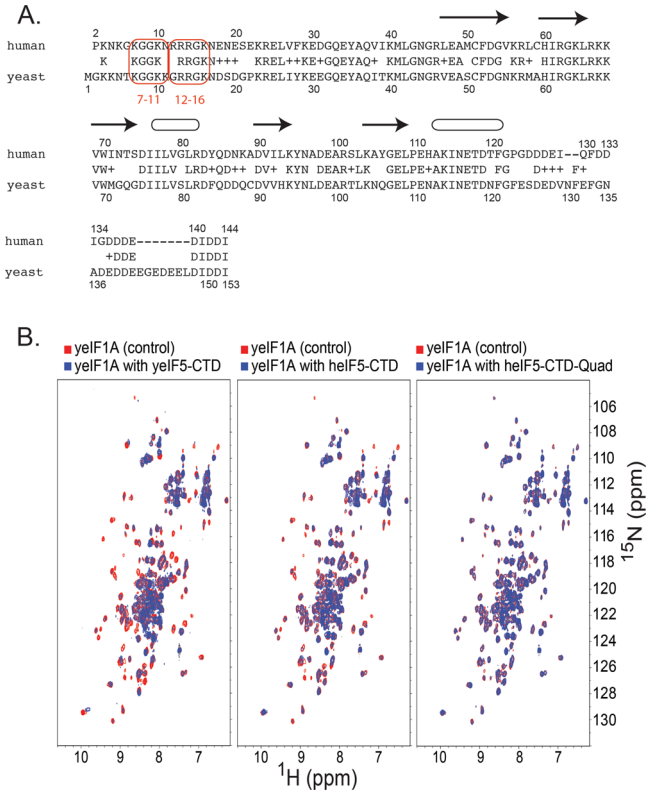


**Figure 3.** Interactions between eIF1A and eIF5-CTD are conserved in yeast and humans and disrupted by the Quad mutation. (A) Amino acid sequence comparison between human and yeast eIF1A. Previously identified mutations on the NTT of yeIF1A are circumscribed in light orange (*tif11*$^{7-11}$ and *tif11*$^{12-16}$). Arrows and ellipses indicate $\beta$-sheet and helical secondary structure, respectively. (B) Overlay of $^{1}$H−$^{15}$N HSQC spectra (left) of 0.2 mM $^{15}$N-labeled yeIF1A alone (red) and in the presence (blue) of 0.4 mM unlabeled wild-type yeIF5-CTD (Tif5-B6) domain. Overlay of $^{1}$H−$^{15}$N HSQC spectra (middle) of 0.2 mM $^{15}$N-labeled yeIF1A alone (red) and in the presence (blue) of 0.4 mM unlabeled wild-type heIF5-CTD domain. Overlay of $^{1}$H−$^{15}$N HSQC spectra (right) of 0.2 mM $^{15}$N-labeled yeIF1A alone (red) and in the presence (blue) of 0.4 mM unlabeled heIF5-CTD-Quad mutant domain (H305D/N306D/E347K/E348K mutant).

complex serves a conserved regulatory role during the scanning process of open PICs.

**eIF1A Forms a Higher-Order Complex with eIF1 and eIF5-CTD.** To examine whether eIF1A forms a higher-order complex with eIF1 and eIF5-CTD and, if so, whether complex formation is mediated by eIF1A-NTT, we performed the GST pull-down assay with yeast proteins (see Figure 4A for GST fusion proteins used). As shown in Figure 4B, full-length GST-yeIF1A or its derivative lacking the CTT (ΔC lacking amino acids 108−153) bound yeIF5-B6 (lanes 6 and 8), but GST-yeIF1A lacking the NTT (ΔN lacking amino acids 1−25) bound it only weakly (lane 10), indicating that the interaction between yeIF1A and yeIF5-CTD depends on yeIF1A-NTT. As shown in Figure 4C, GST-yeIF1A bound yeIF1 and yeIF5-B6 equally well, regardless of whether yeIF1 and yeIF5-B6 were added separately (lanes 7 and 8) or simultaneously (lane 9). Thus, yeIF1A binds simultaneously to yeIF1 and yeIF5-B6, likely forming a higher-order complex. This complex was disrupted by the ΔNTT mutation introduced into GST-yeIF1A (Figure 4C, lane 13). Thus, yeIF1A-NTT mediates these interactions. Interestingly, yeIF1 interacts with yeIF1A (Figure


dx.doi.org/10.1021/bi4009775 | *Biochemistry* 2013, 52, 9510−9518

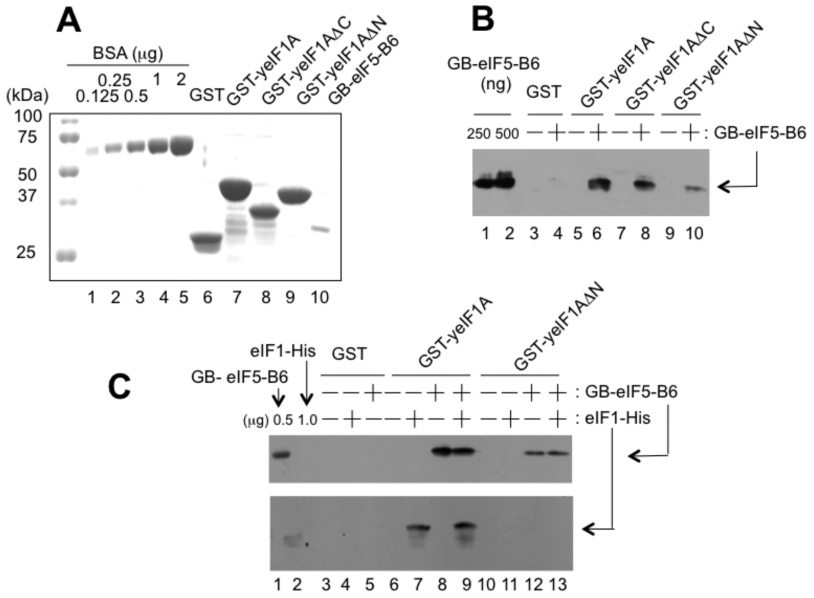


**Figure 4.** eIF1A-NTT mediates interaction with eIF5-CTD and eIF1 in yeast. (A) Coomassie staining of GST fusion proteins used in this study (lanes 6−9). Lanes 1−5 contained BSA standards and lane 10 GB-yeIF5-B6. (B) GST-yeIF1A binds GB-yeIF5-B6. Equal quantities (~5 $\mu$g) of GST or indicated GST fusion proteins were mixed with (+) or without (−) 10 $\mu$g of GB-yeIF5-B6. After being pulled down by glutathione resin and washed, the bound proteins were visualized by immunoblotting with anti-His antibodies. (C) Higher-order complex of yeIF1A, yeIF1, and yeIF5-B6. Equal quantities (~5 $\mu$g) of GST or indicated GST fusion proteins were mixed with (+) or without (−) GB-yeIF5-B6 or with (+) or without (−) eIF1-His (10 $\mu$g each), and the bound proteins were analyzed by immunoblotting, as described for panel B.

4C, lane 7), in contrast to the case in humans (Figure S2 of the Supporting Information). This fact may explain our failure to observe a sufficiently strong eIF1A−eIF5-CTD−eIF1 complex with human proteins.

**Genetic Evidence That eIF1A-NTT Retains eIF1 and eIF5 within the Open Scanning PIC *in Vivo*.** Previous evidence that the NTT of eIF1A contributes to the retention of eIF1 within the PIC prior to the closure on the start codon was presented as follows. *tif11*$^{17-21}$, altering amino acids $_{17}$NDSDG$_{21}$ of the NTT of eIF1A, reduced the amount of eIF1A, eIF1, eIF2, eIF5, and eIF3 in the 43/48S complexes isolated by sucrose gradient velocity sedimentation, in a manner restored by eIF1 overexpression.[25] Consistent with the PIC assembly defect, *tif11*$^{17-21}$ and two other five-alanine substitution mutations, *tif11*$^{7-11}$ and *tif11*$^{12-16}$ (altering $_{7}$KGGKK$_{11}$ and $_{12}$GRRGK$_{16}$, respectively of yeIF1A-NTT), showed a slow growth phenotype in a manner suppressed by eIF1 overexpression (for *tif11*$^{7-11}$ and *tif11*$^{12-16}$, see Figure 5A). These basic residues in the NTT of eIF1A ($_{7}$KGGKK$_{11}$ and $_{12}$GRRGK$_{16}$) are similar to the three K-box regions of the NTD of eIF2$\beta$, which facilitate binding to the CTD of eIF5.

In this study, we focused on the effect of two NTT mutants of yeast eIF1A on *GCN4* expression, because *GCN4* is a sensitive reporter of changes in the stability of the open, scanning PIC. We chose *tif11*$^{7-11}$ and *tif11*$^{12-16}$, since three of the five substituted amino acids in these mutants are arginines or lysines (red boxes in Figure 3A). This resembles the NTD of eIF2$\beta$, which targets a similar binding surface on eIF5-CTD. We first examined the effect on wild-type *GCN4-lacZ* expression (encoded by plasmid p180). The *GCN4* leader region contains four regulatory uORFs. This leader region normally functions to inhibit *GCN4* translation; however, in response to amino acid starvation, the *GCN4* leader region induces *GCN4* translation. Under normal growth conditions, the ribosome that has translated uORF1 stays associated with the mRNA leader, resumes scanning, reinitiates at uORF2, -3, or -4, and dissociates after its translation. Under starvation conditions, eIF2 is phosphorylated, which reduces the level of active eIF2−GTP−Met-tRNA$_i^{Met}$ ternary complexes (TC). This results in the delay of TC binding to the ribosome, wherein the resumed scanning preinitiation complex (PIC) binds to the TC after uORF1 thus bypassing the inhibitory uORFs2−4, allowing initiation at the *GCN4* start codon by the ribosome that has translated uORF1. Mutations that delay TC binding or strengthen TC dissociation from the open PIC allow the bypass of uORFs2−4 by 40S subunits scanning downstream from uORF1 even under normal conditions, increasing the level of expression of *GCN4* (general control derepressed or Gcd$^-$ phenotype). As expected, *tif11*$^{7-11}$ increased the level of *GCN4-lacZ* expression by 20% (Figure 5B, columns 1 and 3), as observed previously with *tif11*$^{17-21}$.[25] Importantly, the increased *GCN4-lacZ* level in *tif11*$^{7-11}$ was significantly diminished by overexpression of eIF1 (Figure 5B, columns 3 and 4). Thus, the weak Gcd$^-$ phenotype of *tif11*$^{7-11}$, suggestive of destabilized TC retention in the open PIC, is due to the weakened PIC retention of eIF1. In the case of *tif11*$^{12-16}$, the most severe slow growth mutant (Figure 5A), the *GCN4-lacZ* level was decreased (Figure 5B, columns 1 and 5) possibly because of the strong bypass of uORF1 and *GCN4* start codons, a condition known to dampen *GCN4* expression.[39] The further decrease in the *GCN4-lacZ* level caused by eIF1 overexpression (Figure 5B, columns 5 and 6) is consistent with the idea that TC retention is also destabilized in this stronger mutant, in a manner restored by increasing the eIF1 occupancy of the PIC.

Next, we examined the effect on *GCN4* expression from a modified construct, pM226. In this plasmid, uORF1 is elongated and overlaps with *GCN4* (Figure 5C). Therefore, *GCN4-lacZ* is translated only when the ribosome has bypassed the uORF1 start codon. As observed with *tif11*$^{17-21}$,[25] both


dx.doi.org/10.1021/bi4009775 | *Biochemistry* 2013, 52, 9510−9518

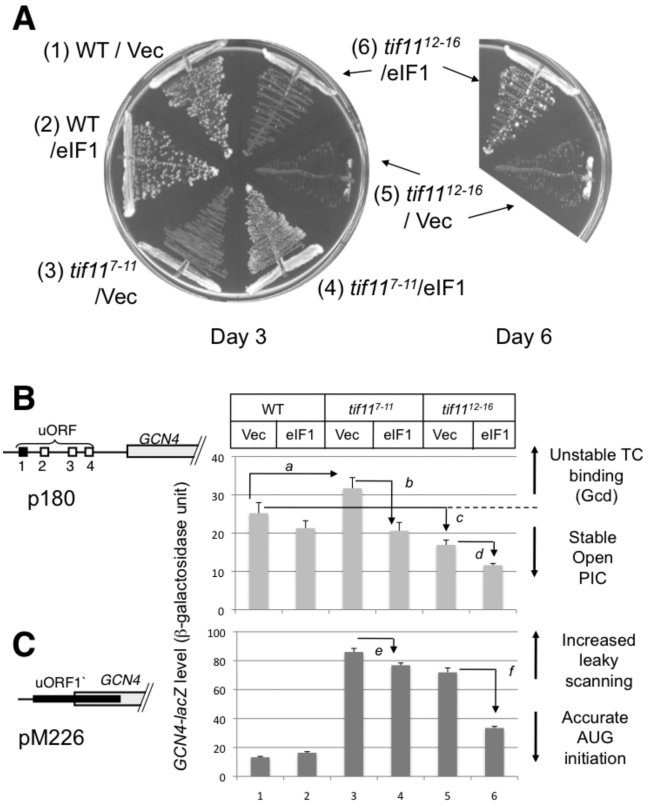


**Figure 5.** Genetic evidence that the lysine- and arginine-rich eIF1A-NTT contributes to stable formation of the open PIC requiring high eIF1 occupancy for its function. (A) In the left panel, *tif11* (yeast eIF1A) mutants (carrying p180) were streaked on plates to verify slow growth phenotypes prior to the assays shown in panel B. The plates were incubated for 3 (left) and 6 (right) days. The six quadrants in the left plate express WT eIF1A and mutants ($tif11^{7-11}$ and $tif11^{12-16}$) paired with either vector alone or high-copy number eIF1. (B and C) *GCN4-lacZ* expression in eIF1A WT and eIF1A-NTT mutations ($tif11^{7-11}$ and $tif11^{12-16}$). Yeast strains used in panel A were doubly transformed with p180 (B) or pM226 (C) carrying *GCN4-lacZ* and with pCF82 (high-copy number eIF1) or a vector control and assayed for *β*-galactosidase. Schematics at the left depict the arrangement of uORFs in the *GCN4* leader region of the *GCN4-lacZ* fusion plasmid employed. *P* values for differences were observed: a, 0.001; b, 0.0005; c, 0.02; d, 0.005; e and f, <0.000001 ($n$ = 8–10).

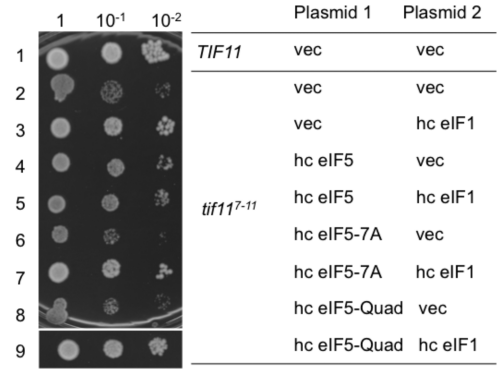


**Figure 6.** Suppression of $tif11^{7-11}$ phenotypes by eIF1 and eIF5 overexpression. Five microliters of a 0.15 $A_{600}$ culture and its 10-fold dilutions of the KAY955 (*TIF11*) or KAY956 ($tif11^{7-11}$) transformant carrying the indicated combinations of the plasmids were spotted onto an SC-ura-trp medium plate and incubated for 4 days at 30 °C. The following plasmids were used: for plasmid 1, YEplac112 (*TRP1*) (vec), YEpW-TIF5 (hc eIF5), YEpW-TIF5-7A (hc eIF5-7A), and YEpW-TIF5-Quad (hc eIF5-Quad), and for plasmid 2, YEplac195 (*URA3*) (vec) and YEpU-SUI1 (hc eIF1).

eIF1A-NTT mutations dramatically increased the level of expression from this plasmid (Figure 5C, columns 1, 3, and 5), indicative of a strong bypass of the uORF1 start codon. Overexpression of eIF1 significantly weakened the strong bypass (Figure 5C, columns 4–6), reinforcing the fact that the leaky scanning arises at least in part because of the weakened retention of eIF1 and attendant dissociation of Met-tRNA$_i$. Together, we provided further evidence that eIF1A-NTT rich in basic residues plays a crucial role in keeping eIF1 in the open, scanning-competent PIC, presumably in part by the interaction of eIF1A with eIF5-CTD.

Having obtained strong evidence that the slow growth phenotypes caused by $tif11^{7-11}$ and $tif11^{12-16}$ are due to unstable anchoring of eIF1 to the open PIC, we next examined whether eIF5 contributes to the stabilization of the open PIC *in vivo*. For this purpose, we overproduced eIF5 in yeast carrying $tif11^{7-11}$. As shown in rows 2 and 4 of Figure 6, the overexpression of wild-type eIF5 partially suppressed the slow growth caused by $tif11^{7-11}$. Importantly, this partial suppression was eliminated when we overexpressed eIF5 mutants carrying *tif5-7A* disrupting its CTD[11,32] (Figure 6, row 6) or *tif5-Quad* weakening the interaction with eIF2*β*, eIF1,[24] and/or eIF1A (Figure 3 and Figure 6, row 8). These results provide *in vivo* evidence of the mutual interaction between eIF5 and eIF1A-NTT via the Quad residues on the CTD surface (Figure S5 of the Supporting Information).

Interestingly, we also observed that eIF5 co-overexpression attenuates the suppression of $tif11^{7-11}$ by hc eIF1, again depending on the intact CTD (disrupted by tif5-7A) or the binding surface of eIF1, eIFA, and eIF2*β* (altered by tif5-Quad) (Figure 6, rows 3, 5, 7, and 9). This suggests that, in the absence of the intact eIF1A-NTT, eIF1 binds eIF5 on the open PIC in a partially competing manner. This is in agreement with the antagonism of eIF5 against the ability of eIF1 to keep the tRNA$_i^{Met}$ anticodon out of the P-site (P*out* state) within the scanning-competent open PIC.[40] Together, the results shown in Figure 6 support the hypothesis that the higher-order complex interaction among eIF1A-NTT, eIF5-CTD, and eIF1 plays a crucial role in maintaining the open conformation of scanning PICs.

## DISCUSSION

A body of biochemical and genetic experiments from yeast studies provides evidence that the NTT of eIF1A, containing the proposed scanning-inhibitor (SI) element, is involved in the closure of the 40S ribosome conformation in response to AUG recognition by Met-tRNA$_i^{Met}$.[25,26] In agreement with this model, eIF1A has been mapped by hydroxyl radical cleavage to the vicinity of the A-site on the 40S subunit, and its NTT lines the bed of the mRNA channel in the direction toward the P-site.[27] The current molecular architecture of the eukaryotic PIC supports the notion that the closure in response to AUG recognition involves the direct interaction of eIF1A-NTT with the 40S subunit P-site, which would stabilize the positioning of the Met-tRNA$_i^{Met}$ in the P-site (P*in* state). In this study, we identified the CTD of eIF5 as an additional partner of eIF1A, which could occur within the 48S PIC in the open conformation, prior to AUG recognition by Met-tRNA$_i^{Met}$.


dx.doi.org/10.1021/bi4009775 | *Biochemistry* 2013, 52, 9510–9518

Our biophysical and genetic analyses provide the first evidence that eIF1A directly binds eIF5. In our previous study with human proteins, we were not able to obtain binding affinities for the eIF1−eIF5-CTD complex, leading us to conclude that other initiation factors assist the CTD of eIF5 in keeping eIF1 in position within the scanning PIC.[24] On the basis of the results of this study, we suggest that one of these other factors includes eIF1A. Because the concentrations used in the interaction assays are much higher than under physiological conditions, the proposed eIF1A−eIF5-CTD−eIF1 complex is weak in both humans and yeast and therefore likely to occur only on the ribosome. However, taking advantage of the *tif11*$^{7-11}$ mutation, which apparently makes the open PIC formation rate-limiting for yeast growth, we provided evidence that the interaction occurs *in vivo* in the open PIC (Figures 5 and 6).

Our finding that the eIF5-Quad mutation (H305D/N306D/E347K/E348K) dramatically weakened the interaction with eIF1A (this study), along with both eIF1 and eIF2$\beta$,[24] strengthens the idea that the altered eIF5-CTD surface, which is in part made of conserved AA boxes,[32] is the "business end" of this factor crucial for PIC assembly. Because eIF1A-NTT and eIF2$\beta$-NTD contain lysine-rich segments along with the evidence that eIF1A and eIF2$\beta$ bind overlapping acidic surfaces on eIF5-CTD (Figure S5 of the Supporting Information), we propose that the putative nexus of eIF1A−eIF5-CTD−eIF1 interactions protects eIF5-CTD from interacting with eIF2$\beta$ prematurely, which would otherwise promote the release of eIF1 and the subsequent closure of the PIC on the start codon (Figure 7). In agreement with this model, the eIF1-binding surface of eIF5-CTD is more extended toward the area including R298−N306 (toward the right in Figure 1D), compared to the eIF1A- or eIF2$\beta$-binding sites (Figure 1C and Figure S5 of the Supporting Information). This would provide sufficient surface area on eIF5 for simultaneous interactions with eIF1 and eIF1A.

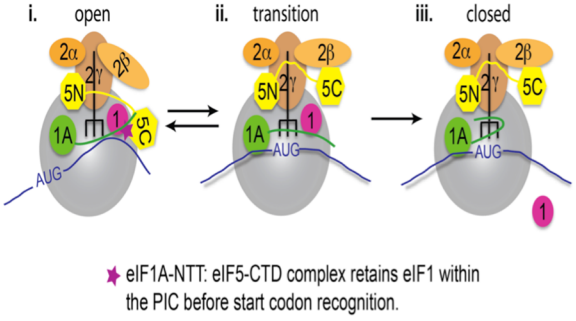


**Figure 7.** Model of events occurring within scanning PICs, wherein the eIF1A-NTT−eIF5-CTD interaction retains eIF1 in position before start codon recognition. (i) During the assembly stage of the open scanning-compatible open PIC, eIF5-CTD interacts with eIF1. It is at this period during scanning that we propose the NTT of eIF1A reaches and binds eIF5-CTD; hence, the eIF1A-NTT−eIF5-CTD interaction effectively keeps eIF1 in position during the scanning process. (ii) The 43S PIC continues to scan the mRNA in an open conformation until start codon recognition. eIF2$\beta$ binds to eIF5-CTD on an overlapping binding surface with eIF1A. eIF2$\beta$ disrupts the interaction of eIF5-CTD with the NTT of eIF1A, which dislodges eIF1 from the PIC. Upon eIF1 ejection, the free phosphate is subsequently released. (iii) The eIF5-CTD−eIF2$\beta$ interaction stabilizes the closed ribosomal conformation of PICs upon start codon selection.

Studies using a yeast reconstitution system (components eIF1, eIF1A, eIF2, eIF5, Met-tRNA$_i^{Met}$, mRNA, and the 40S subunit) provided clues that led us to suggest that eIF1A, along with eIF5-CTD, stabilizes eIF1 within the PIC during the scanning process.[41,42] (1) eIF1 and eIF1A alone can bind to 40S subunits and induce the open conformation, which clears the mRNA channel.[9] A stably bound eIF2-TC (tRNA anticodon is base-paired to the start codon) and eIF1 are mutually exclusive, although eIF1A can clearly promote initial binding of the TC to the 40S subunit.[9] (2) The NTT of eIF1A was mapped to the mRNA channel in the vicinity of the P-site.[27] These findings, when combined, suggest the following. (i) The ability of eIF1A-NTT to stabilize binding of the TC to the P-site is mediated through its direct interaction with Met-tRNA$_i^{Met}$ and the ribosomal P-site, and (ii) eIF1 prevents tRNA accommodation upon start codon recognition. (3) eIF5 was shown to bind to PICs in a fashion antagonistic to eIF1,[40] and more recently, it was shown that this function was mediated through the CTD of eIF5.[41] Because the antagonism is mediated via binding of eIF5-CTD to eIF2$\beta$ to release eIF1 and end the scanning event on the proper start codon,[24] it is reasonable to assume that the eIF2$\beta$-binding site on eIF5-CTD is masked by a PIC component until the closure on the start codon. eIF1A-NTT appears to be bound to the 40S subunit near the P-site in the presence or absence of eIF1 but differently under each condition.[27,36,38] Therefore, binding of eIF1A-NTT to eIF5-CTD (missing in these previous structural studies) in the scanning PIC is plausible and could help stabilize the positioning of eIF1 before start codon recognition.

This model is supported by complementary genetic findings in yeast. eIF1A-NTT mutations altering three consecutive five-amino acid segments exhibited slow growth phenotypes, in a manner suppressed by overexpression of eIF1 *in vivo*[25] (also see Figure 5A). Because the open PIC is characterized as eIF1-loaded PIC, the slow growth phenotype here most likely results from defective loading of eIF1 into the open PIC caused by eIF1A-NTT mutations. Any phenotype suppressed by mass action effects would result from the failure to retain the overproduced component. The first biological evidence suggesting a possible interaction between the NTT of eIF1A and eIF5 was presented in a study showing that a deletion of the first 25 amino acids (NTT) of yeast eIF1A ($\Delta$1−25) inhibited binding of GST-eIF1A to eIF5 in whole cell extracts.[28] Here we verified this interaction using purified proteins (Figure 4). GST-eIF1A was also shown to interact with purified eIF3,[28] which often is copurified with eIF5.[43,44] Because the low affinity of eIF1A for eIF5 does not explain the bridging interaction observed between GST-eIF1A and eIF3,[28] it is likely that eIF3 is involved in indirectly anchoring eIF1 in the open PIC through unidentified interaction with eIF1A, in addition to direct eIF1 anchoring through eIF3c-NTD.[10,45]There is also good evidence that eIF1A promotes the recruitment of eIF5 and eIF3 to the PIC independent of TC binding.[25] While this study links eIF1A to eIF5-CTD and eIF1, other studies link eIF1A-CTT more intimately to eIF2 TC. In strong support of the idea that eIF1A-CTT is the direct binding partner of eIF2 in TC recruitment, eIF1A-CTT deletion mutation ($\Delta$108−153 or $\Delta$C) displays a strong Gcd$^-$ phenotype that can be suppressed by overexpression of eIF2 and tRNA$_i^{Met}$, without disrupting binding of eIF1A-$\Delta$C to the PIC.[46] It was also presumed that the scanning enhancer (SE) elements in eIF1A-CTT directly bind tRNA$_i^{Met}$, preventing it from being positioned tightly in the P-site.[26]


dx.doi.org/10.1021/bi4009775 | *Biochemistry* 2013, 52, 9510−9518

Our biological studies provide additional evidence of the model in which the eIF1A-NTT plays an important role in the retention of eIF1 within PICs before start codon recognition (Figure 5): We showed that (1) the weak Gcd$^-$ phenotype of the eIF1A-NTT mutant *tif*11$^{7-11}$ is suppressed by overexpressing eIF1 and (2) the leaky scanning phenotype of eIF1A-NTT mutant *tif*11$^{12-16}$ is suppressed by overexpressing eIF1. These results indicate that the skipping of uORFs or *GCN4* start codons (which would cause the phenotypes mentioned above) is at least in part due to the weakened interaction between eIF1 and the (open) PIC during the process of scanning. As observed in Figure 4B with the eIF1A ΔN mutation, the substitution mutations in the NTT of eIF1A would weaken the interaction with eIF1 and eIF5-CTD, ultimately weakening the ability to anchor eIF1 within the open PIC. We further propose that the eIF1A−eIF5-CTD interaction normally functions to position eIF1 closer to the P-site via the eIF1−eIF5−eIF1A linkage, such that eIF1 is poised to leave PIC effectively upon anticodon binding of the initiator tRNA to the P-site. If the mutant NTT of eIF1A cannot position eIF1 properly via the CTD of eIF5, then eIF1 cannot be ejected efficiently, allowing the scanning PIC to bypass the AUG start codon.

In conclusion, our results suggest that eIF1A-NTT does not strongly contribute to TC recruitment but contributes to maintaining eIF1 through eIF5-CTD in the open PIC. A breadth of studies on eIF5-CTD suggest that it binds eIF2$\beta$ twice during the pathway of translation initiation: (1) during the formation of the MFC and (2) when the PIC closes on the start codon. During the interim scanning period, our results suggest that eIF1A along with eIF1 masks the acidic eIF2$\beta$-binding site on eIF5-CTD while eIF1 is positioned close to the P-site. Because eIF1A binds weakly to the CTD of eIF5 at a site also targeted by the stronger binder eIF2$\beta$-NTT,[24] it appears that eIF1A binds to eIF5-CTD prior the closure of the PIC as eIF2$\beta$ binding terminates the initiation process.

## ■ ASSOCIATED CONTENT

### Supporting Information

Additional NMR data and the summary diagram. This material is available free of charge via the Internet at http://pubs.acs.org.

## ■ AUTHOR INFORMATION


### Corresponding Authors

*E-mail: gerhard_wagner@hms.harvard.edu. Phone: (617) 432-3213.

*E-mail: kasano@k-state.edu. Phone: (785) 532-0116.

### Present Addresses

[⊥]Michelle A. Markus: R&D Division, Bruker BioSpin Corporation, Billerica, MA 01821.

[¶]Lunet E. Luna: Department of Chemical and Biomolecular Engineering, University of California, Berkeley, Berkeley, CA 94720.

### Author Contributions

[§]R.E.L., H.A., and H.H. contributed equally to this work.



### Funding

This work was supported by National Institutes of Health Grants CA68262 and GM47467 to G.W. and GM64781, Kansas COBRE-PSF Pilot grant, and Innovative Award from KSU Terry Johnson Cancer Center to K.A., and National Institute of Diabetes and Digestive and Kidney Diseases Grant K01-DK085198 to H.A. Use of the National Synchrotron Light Source, Brookhaven National Laboratory, was supported by the U.S. Department of Energy, Office of Science, Office of Basic Energy Sciences, under Contract DE-AC02-98CH10886.

### Notes

The authors declare no competing financial interest.


## ■ ACKNOWLEDGMENTS


We thank Alan Hinnebusch and Assen Marintchev for their useful discussion. We also thank L. Yang and M. Allier (beamline X-9, National Synchrotron Light Source) at Brookhaven National Laboratory (Upton, NY) for assistance with the SAXS experiments.


## ■ REFERENCES


(1) Aitken, C. E., and Lorsch, J. R. (2012) A mechanistic overview of translation initiation in eukaryotes. *Nat. Struct. Mol. Biol. 19*, 568−576.

(2) Asano, K., and Sachs, M. S. (2007) Translation factor control of ribosome conformation during start codon selection. *Genes Dev. 21*, 1280−1287.

(3) Hinnebusch, A. G. (2011) Molecular mechanism of scanning and start codon selection in eukaryotes. *Microbiol. Mol. Biol. Rev. 75*, 434−467.

(4) Pestova, T. V., Borukhov, S. I., and Hellen, C. U. (1998) Eukaryotic ribosomes require initiation factors 1 and 1A to locate initiation codons. *Nature 394*, 854−859.

(5) Pestova, T. V., and Kolupaeva, V. G. (2002) The roles of individual eukaryotic translation initiation factors in ribosomal scanning and initiation codon selection. *Genes Dev. 16*, 2906−2922.

(6) Asano, K., Clayton, J., Shalev, A., and Hinnebusch, A. G. (2000) A multifactor complex of eukaryotic initiation factors, eIF1, eIF2, eIF3, eIF5, and initiator tRNA(Met) is an important translation initiation intermediate in vivo. *Genes Dev. 14*, 2534−2546.

(7) Sokabe, M., Fraser, C. S., and Hershey, J. W. (2012) The human translation initiation multi-factor complex promotes methionyl-tRNAi binding to the 40S ribosomal subunit. *Nucleic Acids Res. 40*, 905−913.

(8) Sonenberg, N., and Hinnebusch, A. G. (2009) Regulation of translation initiation in eukaryotes: Mechanisms and biological targets. *Cell 136*, 731−745.

(9) Passmore, L. A., Schmeing, T. M., Maag, D., Applefield, D. J., Acker, M. G., Algire, M. A., Lorsch, J. R., and Ramakrishnan, V. (2007) The eukaryotic translation initiation factors eIF1 and eIF1A induce an open conformation of the 40S ribosome. *Mol. Cell 26*, 41−50.

(10) Singh, C. R., Watanabe, R., Chowdhury, W., Hiraishi, H., Murai, M. J., Yamamoto, Y., Miles, D., Ikeda, Y., Asano, M., and Asano, K. (2012) Sequential Eukaryotic Translation Initiation Factor 5 (eIF5) Binding to the Charged Disordered Segments of eIF4G and eIF2beta Stabilizes the 48S Preinitiation Complex and Promotes Its Shift to the Initiation Mode. *Mol. Cell. Biol. 32*, 3978−3989.

(11) Asano, K., Hama, C., Inoue, S., Moriwaki, H., and Mizobuchi, K. (1999) The plasmid ColIb-P9 antisense Inc RNA controls expression of the RepZ replication protein and its positive regulator repY with different mechanisms. *J. Biol. Chem. 274*, 17924−17933.

(12) Lorsch, J. R., and Dever, T. E. (2010) Molecular view of 43 S complex formation and start site selection in eukaryotic translation initiation. *J. Biol. Chem. 285*, 21203−21207.

(13) Ivanov, I. P., Loughran, G., Sachs, M. S., and Atkins, J. F. (2010) Initiation context modulates autoregulation of eukaryotic translation initiation factor 1 (eIF1). *Proc. Natl. Acad. Sci. U.S.A. 107*, 18056−18060.

(14) Martin-Marcos, P., Cheung, Y. N., and Hinnebusch, A. G. (2011) Functional elements in initiation factors 1, 1A and 2$\beta$ discriminate against poor AUG context and non-AUG start codons. *Mol. Cell. Biol. 31*, 4814−4831.

(15) Loughran, G., Sachs, M. S., Atkins, J. F., and Ivanov, I. P. (2012) Stringency of start codon selection modulates autoregulation of translation initiation factor eIF5. *Nucleic Acids Res. 40*, 2898−2906.

(16) Conte, M. R., Kelly, G., Babon, J., Sanfelice, D., Youell, J., Smerdon, S. J., and Proud, C. G. (2006) Structure of the eukaryotic initiation factor (eIF) 5 reveals a fold common to several translation factors. *Biochemistry 45*, 4550−4558.
(17) Bieniossek, C., Schutz, P., Bumann, M., Limacher, A., Uson, I., and Baumann, U. (2006) The crystal structure of the carboxy-terminal domain of human translation initiation factor eIF5. *J. Mol. Biol. 360*, 457−465.
(18) Andrade, M. A., and Bork, P. (1995) HEAT repeats in the Huntington's disease protein. *Nat. Genet. 11*, 115−116.
(19) Wei, Z., Xue, Y., Xu, H., and Gong, W. (2006) Crystal structure of the C-terminal domain of *S. cerevisiae* eIF5. *J. Mol. Biol. 359*, 1−9.
(20) Asano, K., Shalev, A., Phan, L., Nielsen, K., Clayton, J., Valasek, L., Donahue, T. F., and Hinnebusch, A. G. (2001) Multiple roles for the C-terminal domain of eIF5 in translation initiation complex assembly and GTPase activation. *EMBO J. 20*, 2326−2337.
(21) Yamamoto, Y., Singh, C. R., Marintchev, A., Hall, N. S., Hannig, E. M., Wagner, G., and Asano, K. (2005) The eukaryotic initiation factor (eIF) 5 HEAT domain mediates multifactor assembly and scanning with distinct interfaces to eIF1, eIF2, eIF3, and eIF4G. *Proc. Natl. Acad. Sci. U.S.A. 102*, 16164−16169.
(22) Das, S., Maiti, T., Das, K., and Maitra, U. (1997) Specific interaction of eukaryotic translation initiation factor 5 (eIF5) with the $\beta$-subunit of eIF2. *J. Biol. Chem. 272*, 31712−31718.
(23) Das, S., and Maitra, U. (2000) Mutational analysis of mammalian translation initiation factor 5 (eIF5): Role of interaction between the $\beta$ subunit of eIF2 and eIF5 in eIF5 function in vitro and in vivo. *Mol. Cell. Biol. 20*, 3942−3950.
(24) Luna, R. E., Arthanari, H., Hiraishi, H., Nanda, J., Martin-Marcos, P., Markus, M. A., Akabayov, B., Milbradt, A. G., Luna, L. E., Seo, H. C., et al. (2012) The C-Terminal Domain of Eukaryotic Initiation Factor 5 Promotes Start Codon Recognition by Its Dynamic Interplay with eIF1 and eIF2$\beta$. *Cell Rep. 1*, 689−702.
(25) Fekete, C. A., Mitchell, S. F., Cherkasova, V. A., Applefield, D., Algire, M. A., Maag, D., Saini, A. K., Lorsch, J. R., and Hinnebusch, A. G. (2007) N- and C-terminal residues of eIF1A have opposing effects on the fidelity of start codon selection. *EMBO J. 26*, 1602−1614.
(26) Saini, A. K., Nanda, J. S., Lorsch, J. R., and Hinnebusch, A. G. (2010) Regulatory elements in eIF1A control the fidelity of start codon selection by modulating $tRNA_i^{Met}$ binding to the ribosome. *Genes Dev. 24*, 97−110.
(27) Yu, Y., Marintchev, A., Kolupaeva, V. G., Unbehaun, A., Veryasova, T., Lai, S. C., Hong, P., Wagner, G., Hellen, C. U., and Pestova, T. V. (2009) Position of eukaryotic translation initiation factor eIF1A on the 40S ribosomal subunit mapped by directed hydroxyl radical probing. *Nucleic Acids Res. 37*, 5167−5182.
(28) Olsen, D. S., Savner, E. M., Mathew, A., Zhang, F., Krishnamoorthy, T., Phan, L., and Hinnebusch, A. G. (2003) Domains of eIF1A that mediate binding to eIF2, eIF3 and eIF5B and promote ternary complex recruitment in vivo. *EMBO J. 22*, 193−204.
(29) Marintchev, A., Frueh, D., and Wagner, G. (2007) NMR methods for studying protein-protein interactions involved in translation initiation. *Methods Enzymol. 430*, 283−331.
(30) Akabayov, B., Akabayov, S. R., Lee, S. J., Wagner, G., and Richardson, C. C. (2013) Impact of macromolecular crowding on DNA replication. *Nat. Commun. 4*, 1615.
(31) Reibarkh, M., Yamamoto, Y., Singh, C. R., del Rio, F., Fahmy, A., Lee, B., Luna, R. E., Ii, M., Wagner, G., and Asano, K. (2008) Eukaryotic initiation factor (eIF) 1 carries two distinct eIF5-binding faces important for multifactor assembly and AUG selection. *J. Biol. Chem. 283*, 1094−1103.
(32) Asano, K., Krishnamoorthy, T., Phan, L., Pavitt, G. D., and Hinnebusch, A. G. (1999) Conserved bipartite motifs in yeast eIF5 and eIF2B$\epsilon$, GTPase-activating and GDP-GTP exchange factors in translation initiation, mediate binding to their common substrate eIF2. *EMBO J. 18*, 1673−1688.
(33) Lee, B., Udagawa, T., Singh, C. R., and Asano, K. (2007) Yeast phenotypic assays on translational control. *Methods Enzymol. 429*, 105−137.
(34) He, H., von der Haar, T., Singh, C. R., Ii, M., Li, B., Hinnebusch, A. G., McCarthy, J. E., and Asano, K. (2003) The yeast eukaryotic initiation factor 4G (eIF4G) HEAT domain interacts with eIF1 and eIF5 and is involved in stringent AUG selection. *Mol. Cell. Biol. 23*, 5431−5445.
(35) Lomakin, I. B., Kolupaeva, V. G., Marintchev, A., Wagner, G., and Pestova, T. V. (2003) Position of eukaryotic initiation factor eIF1 on the 40S ribosomal subunit determined by directed hydroxyl radical probing. *Genes Dev. 17*, 2786−2797.
(36) Lomakin, I. B., and Steitz, T. A. (2013) The initiation of mammalian protein synthesis and mRNA scanning mechanism. *Nature 500*, 307−311.
(37) Rabl, J., Leibundgut, M., Ataide, S. F., Haag, A., and Ban, N. (2011) Crystal structure of the eukaryotic 40S ribosomal subunit in complex with initiation factor 1. *Science 331*, 730−736.
(38) Weisser, M., Voigts-Hoffmann, F., Rabl, J., Leibundgut, M., and Ban, N. (2013) The crystal structure of the eukaryotic 40S ribosomal subunit in complex with eIF1 and eIF1A. *Nat. Struct. Mol. Biol. 20*, 1015−1017.
(39) Hinnebusch, A. G. (2005) Translational regulation of GCN4 and the general amino acid control of yeast. *Annu. Rev. Microbiol. 59*, 407−450.
(40) Nanda, J. S., Cheung, Y. N., Takacs, J. E., Martin-Marcos, P., Saini, A. K., Hinnebusch, A. G., and Lorsch, J. R. (2009) eIF1 controls multiple steps in start codon recognition during eukaryotic translation initiation. *J. Mol. Biol. 394*, 268−285.
(41) Nanda, J. S., Saini, A. K., Munoz, A. M., Hinnebusch, A. G., and Lorsch, J. R. (2013) Coordinated Movements of Eukaryotic Translation Initiation Factors eIF1, eIF1A and eIF5 Trigger Phosphate Release from eIF2 in response to Start Codon Recognition by the Ribosomal Pre-initiation Complex. *J. Biol. Chem. 88*, 5316−5329.
(42) Maag, D., Algire, M. A., and Lorsch, J. R. (2006) Communication between eukaryotic translation initiation factors 5 and 1A within the ribosomal pre-initiation complex plays a role in start site selection. *J. Mol. Biol. 356*, 724−737.
(43) Asano, K., Phan, L., Anderson, J., and Hinnebusch, A. G. (1998) Complex formation by all five homologues of mammalian translation initiation factor 3 subunits from yeast *Saccharomyces cerevisiae*. *J. Biol. Chem. 273*, 18573−18585.
(44) Phan, L., Zhang, X., Asano, K., Anderson, J., Vornlocher, H. P., Greenberg, J. R., Qin, J., and Hinnebusch, A. G. (1998) Identification of a translation initiation factor 3 (eIF3) core complex, conserved in yeast and mammals, that interacts with eIF5. *Mol. Cell. Biol. 18*, 4935−4946.
(45) Valasek, L., Mathew, A. A., Shin, B. S., Nielsen, K. H., Szamecz, B., and Hinnebusch, A. G. (2003) The yeast eIF3 subunits TIF32/a, NIP1/c, and eIF5 make critical connections with the 40S ribosome in vivo. *Genes Dev. 17*, 786−799.
(46) Fekete, C. A., Applefield, D. J., Blakely, S. A., Shirokikh, N., Pestova, T., Lorsch, J. R., and Hinnebusch, A. G. (2005) The eIF1A C-terminal domain promotes initiation complex assembly, scanning and AUG selection in vivo. *EMBO J. 24*, 3588−3601.